University of Baghdad
College of Engineering
JE
JOURNAL OF ENGINEERING

Journal of Engineering

journal homepage: www.jcoeng.edu.iq

Volume 32 Number 7 July 2026

Assessing The Synergistic Impact of Urban Morphology and Air Pollution on SUHI Using Multi-Sensor Data Fusion and Machine Learning

Raghad Hadi Hasan

Department of Surveying Engineering, College of Engineering, University of Baghdad, Baghdad, Iraq

ABSTRACT

Urban environments face serious climate challenges due to rapid urban expansion, exacerbating the surface urban heat island (SUHI) phenomenon. This study proposes a hybrid framework based on Multi-sensor Fusion technology within the cloud computing environment of the Google Earth Engine platform to overcome the limitations of single data sources. Focusing on Baghdad from 2018 to 2023, Multi-spectral, radar, and atmospheric satellite datasets (Landsat 8/9, Sentinel-1, Sentinel-2, Sentinel-5P) were integrated to accurately extract morphological and environmental variables at the standardized residential neighborhood scale. A spatiotemporal model was constructed based on the random forest algorithm to evaluate the relative impact of urban drivers. The model showed high predictive efficiency, achieving a coefficient of determination (R^2 = 0.842) and a root mean square error (RMSE = 1.007°C). The results revealed that urban morphology (NDBI contribution of 29.43%) and air quality degradation (NO_2 contribution of 25.38%) are the main drivers of surface warming. This study provides empirical evidence of the synergistic polluted-heat-dome effect, offering a geospatial tool for urban planners to adopt sustainable, climate-resilient mitigation strategies in arid metropolitan areas.

Keywords: Remote sensing analysis**,** Surface Urban Heat Island (SUHI), Geospatial big data, Image processing, Random Forest.

1. INTRODUCTION

In the 21st century, the world faced a growing environmental challenge in the form of rapid urbanization, which directly led to radical transformations in the physical characteristics of the Earth's surface **(Al-Sabbagh and Al-Lami, 2021)**.In cities in arid and semi-arid regions, such as the Iraqi capital, Baghdad, this growth was not limited to horizontal expansion but was also accompanied by a structural change in "urban morphology" through the replacement of natural vegetation with concrete blocks and solid asphalt surfaces with high thermal capacity. This structural shift traps solar energy during the day and re-radiates it at night, leading to an exacerbation of the surface urban heat island (SUHI) phenomenon, which

*Corresponding author
Peer review under the responsibility of University of Baghdad.
https://doi.org/10.31026/j.eng.2027.07.12

Article received: 15/05/2026
Article revised: 06/06/2026
Article accepted: 06/06/2026
Article published: 01/07/2026

is one of the most prominent features of local climate change **(Oke et al., 2017; Zhou et al., 2021; Wang et al., 2023)**.

The combined influence of urban form and air quality is one of the complexities of urban climates that pose a challenge to major cities. The tall and densely packed buildings not only absorb heat but also act as mechanical barriers, which prevent the dispersal of gaseous pollutants produced by human activities, particularly nitrogen oxides (NO_2) **(Ulpiani, 2021)**. From a scientific perspective, the accumulation of these pollutants leads to the creation of what is known as a polluted heat dome, that is where local greenhouse gases act as a blanket that traps terrestrial radiation, creating a vicious cycle of mutual warming between chemical pollution and the urban structure **(Fan et al., 2023; Zhang et al., 2024; Zhang and Li, 2025)**.

Despite the abundance of studies addressing surface urban heat islands (SUHI), most previous literature has focused on simple regression analysis or single-factor analysis. For example, **(Al-Hashemi et al., 2022)** focused solely on Landsat data to assess temperatures in Baghdad, without considering complex building morphology. In the context of machine learning, **(Belgiu et al., 2016)** demonstrated the efficiency of randomized forests but did not integrate radar data to assess urban roughness. Regarding pollution, **(Ulpiani, 2021)** discussed the relationship between pollutants and heat as two separate pathways. A significant knowledge gap exists in the absence of synergistic modeling that integrates optical, radar (SAR), and atmospheric monitoring (TROPOMI) data into a single framework. Understanding these complex relationships requires a sophisticated technical approach that goes beyond traditional analyses. This is where the importance of "multi-sensor fusion" comes in. Recent geospatial literature has witnessed a strong trend toward employing multi-sensor fusion techniques to understand the thermal dynamics of cities. In this regard, **(Hoang and Nguyen, 2025)** developed a spatial framework based on machine learning algorithms and fused data to predict the intensity of heat islands, demonstrating the efficiency of advanced predictive models in explaining 90% of the thermal variability associated with morphological changes. In a related vein, the study by **(Haseeb et al., 2026)** went beyond physical surface analysis to demonstrate a synergistic interaction between air pollution and rising surface temperatures. Satellite data confirmed that pollutants exacerbate thermal stress in a non-linear manner. Building on these findings, our current research aims to bridge the gap in understanding the interplay between complex structural morphology and pollution concentrations, and their combined impact on Baghdad's local climate By combining radar (SAR) data, capable of describing three-dimensional morphological roughness, with optical, thermal, and chemical data obtained from the Sentinel and Landsat satellite series, we can build a holistic model that tracks temporal and spatial changes with high accuracy **(Gao et al., 2022; Hafner et al., 2024)**.

The study aims to provide an integrated framework based on machine learning algorithms within the Google Earth Engine environment, by firstly with the goal of analyzing and evaluating the synergistic interaction between urban morphology and air pollution in the city of Baghdad. Through this approach, the study seeks to determine the relative weight of each of these factors and their combined impact on shaping the microclimate of the city, thus providing a predictive database that supports decision-makers in formulating planning strategies that ensure the sustainability and climatic resilience of the urban environment.

2. METHODOLOGY

2.1. Study Area and Data Sources

2.2.1. Description of the Study Area

The Iraqi capital, Baghdad, was chosen as the area of study **Fig.1** which represents a vivid model of major urban centers in arid and semi-arid regions that suffer from the pressures of intensive urban expansion. The city is located within the alluvial plain in central Iraq and is characterized by an arid desert climate according to the Köppen-Geiger classification, where it experiences sharp temperature variations and harsh climatic conditions that contribute to the complexity of urban climate physics **(Salman et al., 2021; Al-Hashemi et al., 2022)**. The rapid population growth and haphazard urban sprawl that the city has witnessed in recent decades have made it a fertile environment for studying the complex interactions between urban morphology and the phenomenon of surface warming.

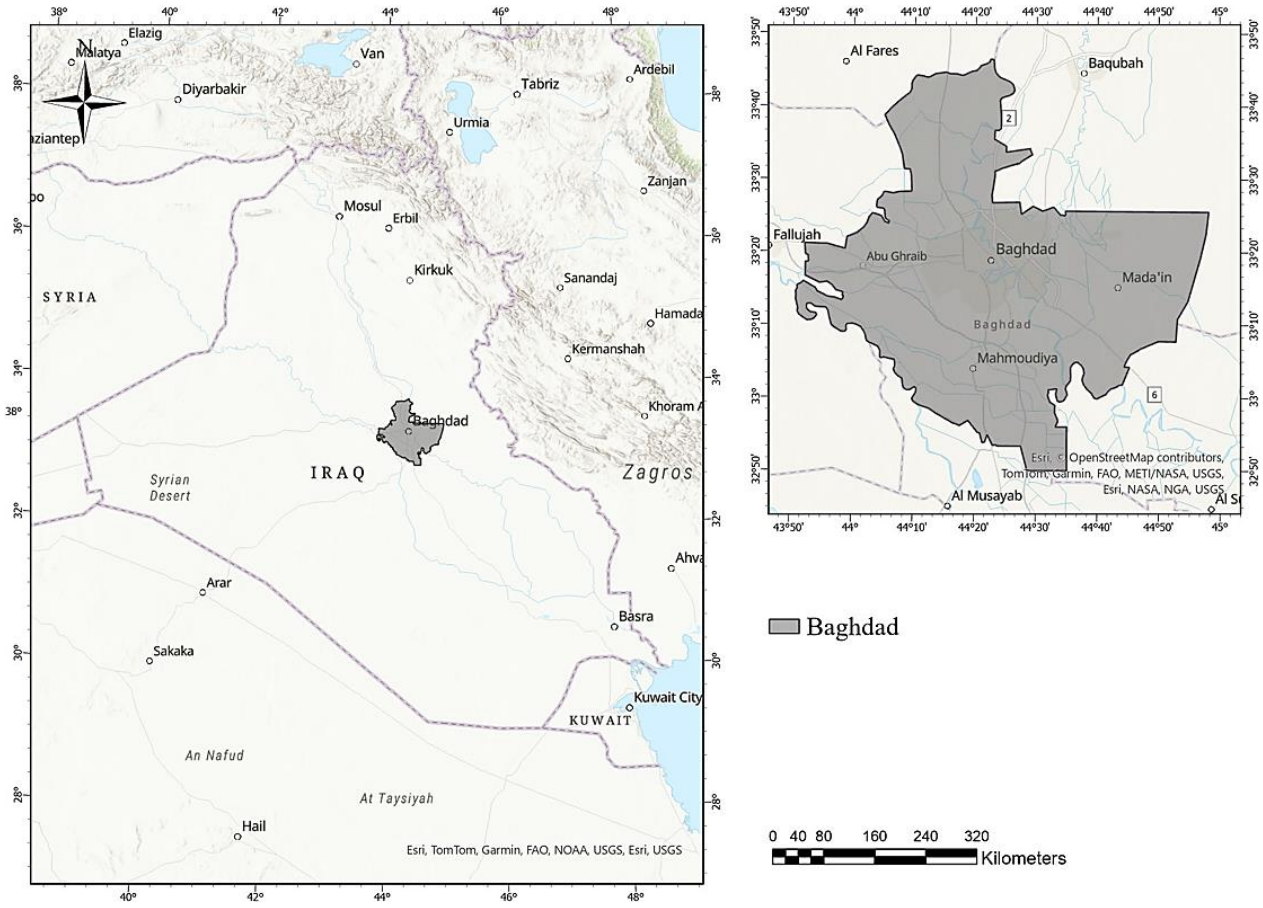

Figure 1. Location map of the study area (Baghdad City, Iraq).

2.2.2. Data Sources and Computing Platform

For the purpose of processing Big Data and analyzing time series data for the period from 2018 to 2023, the cloud computing capabilities of the Google Earth Engine (GEE) platform were relied upon. This enables the processing of geospatial data at planetary scales without the need for local storage **(Gorelick et al., 2017; Tamiminia et al., 2020; Liu et al., 2024)**. Data from four space missions by the US space agency (NASA) and the European Space Agency (ESA) were combined as follows:

1. Landsat 8/9 (TIRS) mission: Thermal Infrared Sensor imagery was called in to extract land surface temperatures (LST) with a spatial resolution of 100 meters (Renamed to 30 meters), it is the primary reference data for assessing heat islands **(Parastatidis et al., 2021)**.
2. Sentinel-2 (MSI) mission: High-resolution multispectral imaging (10-20 meters) was used to calculate the axial environmental indicators this includes the Normalized Difference vegetation index (NDVI), the Normalized Difference built-up index (NDBI) **(Jasim et al., 2025)** as well as calculating the surface reflectance coefficient (Albedo), which is an important physical constant in the surface energy budget **(Tuholske et al., 2021)**.
3. Sentinel-1 (SAR) mission: For the purpose of characterizing three-dimensional urban morphology, dual-polarization synthetic aperture radar (VV+VH) data were used. These active sensors provide accurate measurements of surface roughness and urban volume (SAR_Volume). It is a technology that surpasses optical sensors in its ability to penetrate air obstacles and provide information about the city's geometric structure **(Gao et al., 2022; Sun et al., 2022)**.
4. Sentinel-5P (TROPOMI) mission: Data from this atmospheric monitoring satellite were used to extract nitrogen dioxide (NO_2) column concentrations. The TROPOMI sensor is characterized by high accuracy, enabling it to track emissions resulting from traffic and industrial activity within urban areas with unprecedented precision **(Kaplan et al., 2021; Wang et al., 2023)**.

2.2 Preprocessing and Spatial Harmonization

Cloud masking techniques and monthly balanced average calculations were applied to ensure that the time series were free from any seasonal bias and to address the sharp variation in spatial resolution between multiple sensors (ranging from the high spatial resolution of Sentinel-2 images to the low resolution of Sentinel-5P data). The Grid-based Harmonization methodology was adopted. The spatial scale, Spatial Resampling, of all variables was reset and projected onto an intermediate spatial grid. The Intermediate Spatial Grid is compatible with the morphology of the city.

To ensure the quality of the input data and its freedom from atmospheric distortions the Landsat 8/9 and Sentinel-2 images underwent advanced radiometric and geometric processing within the Google Earth Engine (GEE) environment after this the Cloud masking algorithms were applied based on the available quality packages, which the QA_PIXEL package was adopted for Landsat images and the QA60 package for Sentinel-2 images to isolate clouds and shadows with high accuracy. And for Atmospheric Correction, the ready-made Surface Reflectance products were used that corrected via the LaSRC algorithm for Landsat and the Sen2Cor algorithm for Sentinel-2 **(Gorelick et al., 2017).**

Regarding the Sentinel-1 radar (SAR) data, the standard processing sequence adopted for Ground Detection Range (GRD) products was traced in a GEE environment **(Mullissa et al., 2021),** which included five key phases:

- Applying an Orbit File to correct geometric errors in the path.
- Thermal noise removal to reduce distortions at the edges of the scene.
- Radiometric Calibration to convert digital amplitude values to the backscatter coefficient of sigma zero (σ^o) in decibels (dB).
- Geometric correction of terrain (Orthorectification) using a digital elevation model (SRTM 30m).

- Applying a speckle filter using a refined Lee filter with a (5*5) window range to reduce radar speckle without losing fine urban details of building edges **(Filipponi, 2019).**

Adopting this intermediate spatial scale is considered ideal and scientifically justified for deducing the effects of urban morphology at the neighborhood scale rather than the individual pixel level. Furthermore, this measure effectively contributes to filtering and reducing the inherent speckle noise of Synthetic Aperture Radar (SAR) data, ensuring a reduction in uncertainty and creating a precise systematic balance for the spatiotemporal modeling process, refer to **Fig. 2.**

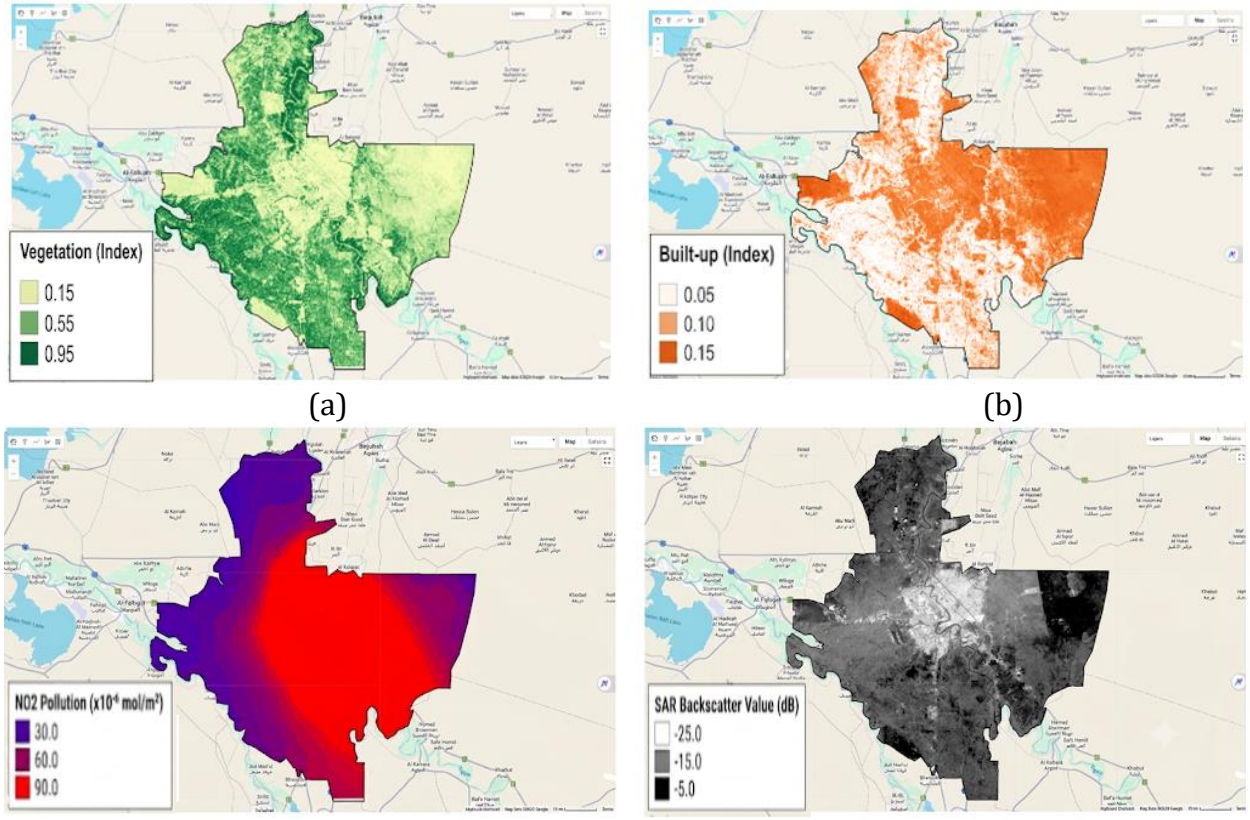

Figure 2. Spatial distribution of the standardized urban and environmental variables: (a) NDVI, (b) NDBI, (c) NO_2 concentration, and (d) SAR Volume.

The choice of the intermediate spatial network with an accuracy of 30 meters is attributed to specific physical and statistical justifications. This scale geographically represents the most suitable Neighborhood Scale for simulating urban climate dynamics without losing the thermal accuracy derived from the Landsat reference sensor. To address the sharp variations in sensor accuracy and mitigate uncertainty errors. For resampling the NO_2 gas from the Sentinel-5P sensor, we adopted the Cubic Convolution algorithm. This ensures continuous statistical smoothing that prevents spatial bias and reduces the phenomenon of interpolation artefacts. Our results from the merging of pixels of varying sizes, which achieves a systematic balance that ensures the preservation of the physical meaning of the integrated morphological and environmental indicators. **Table 1** presents the results of the co-registration verification between the multiple sensors used in our study. The root mean squared error (RMSE) values, which registered levels below one pixel (less than 0.25 pixels for all layers), indicate successful spatial harmonization. This reduction in pixel offset is

essential for ensuring the reliability of the data fusion process, as it guarantees that the variables extracted from Sentinel-5P and Sentinel-1 accurately represent the same geographic locations thermally observed by Landsat, thus reducing spatial noise in subsequent modeling.

Table 1. Spatial alignment accuracy criteria between different sensors

Data type	Reference sensor	Method of resampling	RMSE (pixels)
Sentinel-2 (NDVI/NDBI)	Landsat 8/9	Bilinear Interpolation	0.12
Sentinel-1 (SAR Volume)	Landsat 8/9	Nearest Neighbor	0.18
Sentinel-5P (NO_2)	Landsat 8/9	Cubic Convolution	0.24

Surface temperatures (LST) were extracted from the thermal band 10 of Landsat 8/9 by applying the emissivity-corrected single-channel algorithm according to the following mathematical steps **(Ermida et al., 2020)**.
First: The numerical values (*DN*) were converted to spectral radiation (L_λ) at the top of the atmosphere via Eq. (1)

$$L_\lambda = M_L * DN + A_L \quad (1)$$

Where M_L is the multiple scaling factor of the range ($3.342* 10^{-4}$), and A_L is the addition factor (0.1).

Second: Converting spectral irradiance to spectral luminosity temperature (T_B) in Kelvin (K) using the Landsat thermal calibration constants via Eq. (2)

$$TB = \frac{K2}{In(\frac{K1}{L\lambda}+1)} \quad (2)$$

Where the constants are for Landsat 8 (K1 = 774.88 and K2 = 1321.07 W/(m^2.sr.µm), and for Landsat 9 (K1 = 799.02 and K2 = 1329.03 W/(m^2.sr.µm)
Third: Calculating the final surface temperature (LST) in degrees Celsius (C^0) by correcting the brightness values based on the surface emissivity (€) **(Sobrino et al., 2004)** via Eq. (3)

$$LST = \left(\frac{TB}{1+\left(\frac{\lambda.TB}{\rho}\right)In(€)}\right) - 273.15 \quad (3)$$

Where λ is the effective wavelength of the 10 band (10.89µm), and K = $1.438*10^{-2}$ (where ρ=*h* * *c/o* where *h* is Planck's constant, c is the speed of light, and o is Boltzmann's constant). The emissivity € was calculated based on the Vegetation Index Threshold Method (NDVI Threshold Method) to differentiate between exposed soil ($€_s$ = 0.966) and full vegetation cover ($€_v$ = 0.985) according to the vegetation fraction (P_v) via Eq. (4)

$$Pv = \left(\frac{NDVI-NDVImin}{NDVImax-NDVImin}\right)^2 \quad (4)$$

$$€ = €_v . Pv + €_s . (1- Pv) + d_€ \quad (5)$$

Where $d_€$ expresses the geometric roughness coefficient of buildings and urban volume, in Eq.(5) estimated at 0.005 for dense urban fabric **(Sobrino et al., 2004)**.

2.3 Spatial Modeling and Performance Evaluation

The Random Forest (RF) algorithm was employed as a non-parametric machine learning model to decipher the complex and nonlinear relationships between environmental and morphological variables on the one hand and land surface temperature (LST) on the other. This algorithm was specifically chosen for its high ability to handle excessive multicollinearity among urban indicators **(Kumar et al., 2024)** and for its robustness against the problem of overfitting **(Maxwell et al., 2021; Zhang et al., 2024; Jasim et al., 2025)**.

Model preparation: A dense spatial random sampling was generated covering all topographic and thermal variations of the study area, and the dataset was statistically divided into 70% for the training set to build the model, and 30% for the testing set to independently verify its accuracy. We used to ensure the highest predictive efficiency and avoid the problem of overfitting; the Random Forest algorithm underwent a comprehensive hyperparameter tuning process using grid search with cross-validation (GRI). The optimal computational properties of the final model in the GEE environment were determined based on the following parameters **(Tyralis et al., 2019; Maxwell et al., 2021)**. We set the number of decision trees (n_estimators) to 100 trees because that is the limit that showed complete stability in reducing the mean squared error without excessive consumption of cloud memory. Also, we set the Maximum random features (variables PerSplit) mathematically to equal the square root of the total number of independent variables because that enhances statistical variability between trees and reduces their interrelationship. Minimum Leaf Population Size we set at 5 samples to prevent the branching of trees to infinitesimal levels that may represent statistical noise rather than true patterns. Maximum tree depth (maxDepth) is limited to 15 to ensure a balance between complex explanatory power and the model's generalization power on independent data. In order to demonstrate the superior efficiency of the Random Forest (RF) model, we conducted this research by creating and comparing two alternative models under the same computational conditions and optimal parameters, which were the Extreme Gradient Boost Algorithm (XGBoost) and Supporting Vector Machines (SVM).

2.4. Feature Importance Analysis

In order to establish a deeper understanding of the role that morphological and environmental factors play in shaping the surface heat island pattern, our study relied on the permutation importance algorithm to assess the specific weight of each independent variable. In this methodology, we aim to break the black box barrier in machine learning models **(Molnar, 2020)** by measuring the predictive sensitivity of the model to each variable individually. This mathematical mechanism is based on the Increase in Mean Squared Error (IncMSE%) criterion, where a random shuffling process is performed on the values of a particular variable while keeping the other variables constant, and then the extent of the deterioration in the accuracy of the prediction is calculated. From a physical and statistical perspective, any sharp increase in the standard error after the switching process reflects the pivotal value of that variable in explaining spatial thermal variability, making it a key driver in the city's climate system **(Gao et al., 2022; Shrestha et al., 2022)**. In this study, in order to identify the most influential factors in the surface urban heat island phenomenon, we followed an analytical approach to obtain accurate results by precisely isolating and identifying the intermediate variables.

3. RESULTS, ANALYSIS, AND DISCUSSIONS

3.1 Model Performance and Statistical Reliability

The results in our study of the comparative evaluation based on decagonal cross-validation show a clear statistical superiority of the Random Forest (RF) algorithm in simulating and interpreting the spatial variation of land surface temperatures (LST). **Table 2** presents a detailed quantitative comparison between the three tested models based on independent validation data.

Table 2. Comparative performance metrics of different machine learning models based on ten-fold cross-validation.

Model	10-Fold R^2	RMSE (°C)	MAE (°C)
Random Forest (RF)	0.842	1.007	0.785
XGBoost	0.821	1.120	0.840
Support Vector Machine (SVM)	0.765	1.340	0.995

Table 2 shows that the (RF) model achieved the highest coefficient of determination (R^2 = 0.842) and the lowest error rate (RMSE = 1.007 °C). This reflects its ability to handle complex nonlinear and multicollinear relationships between urban morphological variables and pollution, thus outperforming the XGBoost and SVM algorithms. To verify the spatial stability of the model, a residual analysis was performed, as shown in the cross-validation results. The fact that 92% of the error values were within one standard deviation (±1.5 °C) indicates that the model possesses high generalization power across the diverse urban fabric of Baghdad. From this result, the homoscedasticity of errors confirms the model's lack of spatial bias, which makes it a reliable tool for predicting temperatures even in organisms with extreme morphological characteristics and enhancing the reliability of the resulting thermal maps.

In our study, we can see outputs of the Random Forest (RF) algorithm demonstrated high statistical reliability and predictive efficiency in simulating the spatial variation of land surface temperatures (LST) within the study area. As shown in the scatter plot **Fig. 3,** the point distribution of the Validation Set data shows a strong positive linear correlation, with the predicted values being closely centered around the ideal regression line.

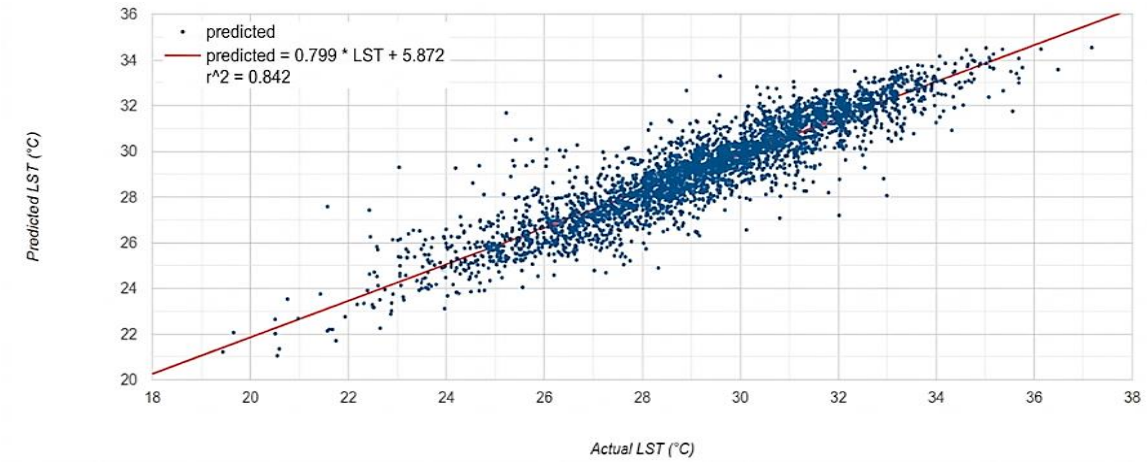

Figure 3. The dispersion diagram illustrates the linear relationship between the actual land surface temperatures (Actual LST) and the values predicted by the model for the validation data.

When statistically interpreting the results of our research, the model shows high predictive efficiency (R^2 = 0.842), indicating that the selected independent variables are capable of explaining more than 84% of the variance in heat islands. Furthermore, the model recorded a very low value for the root mean square error (RMSE = 1.007 °C), a small margin of error that confirms the validity of the methodology used and proves the high spatial homogeneity of the data after applying the Spatial Harmonization process.

The spatial distribution of the model outputs visually corresponds to these statistical measures, as **Fig. 4** shows a remarkable spatial match between the actual land surface temperatures extracted from satellites and those predicted by the Random Forest (RF) model. This match is clearly evident in the accuracy of monitoring and identifying the hot thermal hotspots located within dense urban areas **(Ren et al., 2023)**.

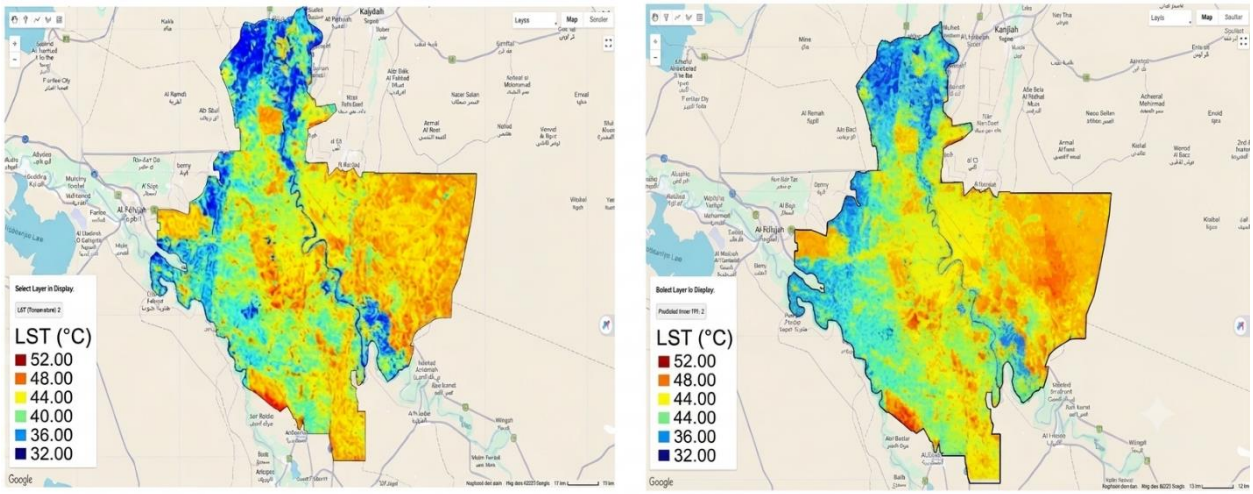

(a) (b)

Figure 4. Spatial comparison between (a) Actual LST derived from Landsat 8/9 and (b) Predicted LST generated by the Random Forest model.

3.2 Analysis of the Relative Importance of Urban Drivers

To assess the extent to which each environmental and urban variable contributes to the increase of the surface heat island phenomenon, the relative importance of the variables resulting from the model was determined, as shown in the bar chart **Fig. 5**. The outputs reveal a strategic divergence in the drivers of warming; urban morphology, represented by the Normalized Difference Built -up Index (NDBI), dominated as the primary factor and the strongest main driver with a contribution of (29.43%). The most prominent scientific paradox presented by this model is the rise of air pollutants (NO_2) to second place as a decisive factor, with a percentage of (25.38%), thus surpassing the cooling role of the Normalized Difference vegetation index (NDVI), which came in third place with a percentage of (23.63 %). Meanwhile, surface roughness represented by radar data (SAR_Volume), contributed (21.54 %).

This systematic order of importance quantitatively demonstrates that the exacerbation of heat islands is not solely dependent on two-dimensional concrete expansion, but is synergistically and directly affected by the deterioration of air quality and the three-dimensional geometric structure of the city **(Chen et al., 2023)**.

To analyze the driving forces of surface warming, **Table 3** presents the statistical correlation coefficients between the independent variables and land surface temperature (LST). The strong positive correlation value of the structural index (NDBI=+0.78) stands out as quantitative evidence of the pivotal role of concrete masses in heat absorption. Conversely, the positive correlation of NO_2 reveals the contribution of air pollution to enhancing local global warming. This variation in correlation values (the positive correlation between buildings and pollution, and the negative correlation with plant food) proves the validity of the study's hypothesis regarding the synergistic effect of morphology and pollution in the formation of surface urban heat islands.

Table 3. Pearson correlation matrix (r) between independent variables and surface temperature.

Variable	LST (temperature)	Physical explanation
NDBI	+0.78	Strong positive correlation (buildings increase heat)
NO_2	+0.65	Moderate positive correlation (pollution contributes to global warming)
NDVI	-0.54	Inverse relationship (plants act as a natural coolant)
SAR_Volume	+0.49	Direct correlation (building mass hinders ventilation)

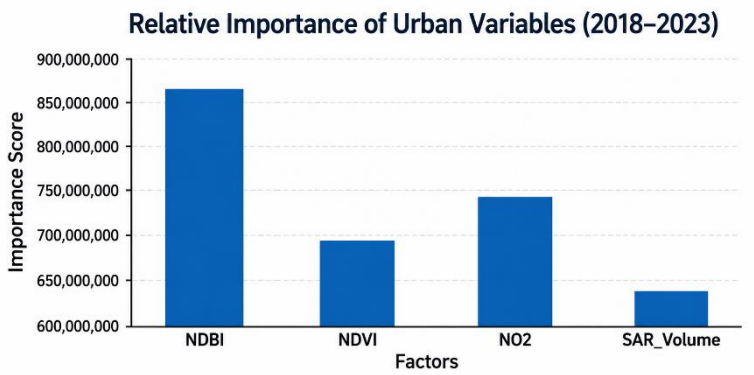

Figure 5. Relative importance (%) of environmental and morphological variables in influencing surface temperatures (LST) using a random forest model.

3.3 Synergistic Interaction between Morphology and Pollution

The study's findings go beyond a single explanation of the factors, revealing a complex synergistic pattern between air pollution and urban form. Through the intersection of thematic maps which it became clear that the 'hottest' areas in Baghdad (those exceeding 45°C) were not only associated with high building density (NDBI > 0.3) but were also the same areas suffering from air stagnation that led to high concentrations of pollutants (NO_2 > 150 umol/m^2). From a precise physical and atmospheric perspective, the spatial correlation between nitrogen dioxide concentrations (NO_2) and land surface temperature increases (LST) should be interpreted as a synergistic relationship governed by complex feedback mechanisms, rather than an isolated linear causality. In this kinetic framework, NO_2 plays a dual role; it acts as an indirect spatial proxy for the intensity of anthropogenic heat fluxes emitted from the exhausts of vehicles and local power plants in Baghdad, which release high perceived heat in conjunction with greenhouse gases. Secondly, the concentration of gaseous pollutants over densely populated urban areas causes a modification of the local radiation balance as particles and gases contribute to increasing the optical depth of the atmosphere

surrounding the city, which leads to the absorption and trapping of long-wave terrestrial radiation emitted from concrete blocks at night and inhibition of nocturnal Radiative Cooling. Thus, the term polluted heat dome is introduced here as a descriptive and dynamic framework that embodies the combined thermal-chemical interaction, where morphological properties support air stagnation, while pollution, in turn, hinders heat dissipation.

3.4 Spatiotemporal Development and Comparative Analysis (2018-2023)

Time-based analysis spanning 2018 to 2023 revealed a continuous linear upward trend in the intensity of surface urban heat island (SUHI) in Baghdad, with an annual growth rate of 0.15°C. This trend is statistically synchronous with the growth in building density and the rise in NO_2 gas concentrations .When assessing seasonal variability, the results showed a sharp variation. The intensity of heat islands and the synergistic relationship between morphology and pollution reach their peak during the summer, with an average urban-rural heat gap of 4.8 °C.As a result of the prevailing atmospheric stability and calm winds, compared to winter, when the temperature gap decreases to 1.2°C due to the dynamic activity of the air. Regarding the evolution of hotspots, it became clear that the city's thermal core witnessed a geographically concentrated expansion in the commercial activity centers on both the Karkh and Rusafa sides. Isolated thermal hotspots transformed into geographically connected and extended thermal zones due to the merging of impermeable surfaces and buildings. Comparing these findings with previous literature, the general trends identified align with regional studies published in arid environments **(Salman et al., 2021; Al-Hashemi et al., 2022).** However, the current proposed methodology was distinguished by its higher ability to explain 84.2% of the thermal spatial variation by integrating the chemical and radar dimensions. That will be supported by recent international trends, such as **(Fan et al., 2023),** which emphasize the increasing environmental stress in major cities as a result of the dynamic interaction between the urban infrastructure and the air quality.

4. CONCLUSIONS

Based on the results found in our study that align with modern theories in urban climate physics, the analytical effectiveness of the multi-sensor integration approach. The scientific implications of the results can be summarized in the following points:

- Two-dimensional morphology: The Normalized Difference Built-up Index (NDBI) emerged as the most important driver (29.43%), which physically translates the negative impact of urban sprawl where impervious surfaces and high-heat-capacity concrete act as reservoirs for solar radiation, limiting the city's evaporative cooling.
- The phenomenon of the polluted heat dome: The rise of gaseous pollutants (NO_2) to second place (25.38%) is the most notable finding of the study. It provides quantitative evidence of the synergistic interaction between deteriorating air quality and warming urban emissions, which act as a blanket that traps long-wave terrestrial radiation, hindering heat dissipation day and night.
- Three-dimensional structure and spatial approach: The use of the intermediate spatial network proved efficient in integrating radar roughness data (SAR_Volume). The contribution of this variable (21.54%) confirms that the vertical distribution of building masses plays a crucial role in obstructing urban ventilation pathways, a role that is as important as the absence of vegetation cover.

The planning recommendations to activate the practical value of the spatial outputs were transformed into three specific implementation paths for Baghdad.
Spatial Mitigation Priorities that Directing environmental investments immediately towards the targeted red zones in the study maps (such as the crowded business centers in Karkh and Rusafa) which where the high Normalized Difference Built-up Index (NDBI > 0.3) intersects with high pollution energy (NO_2 > 150 umol/m^2)By mandating the replacement of traditional surfaces with materials that have a high solar reflectance coefficient such (Albedo > 0.6) to break up the thermal core**.** Urban Planning Scenarios, which Implementing the Urban Ventilation Corridors mechanism in neighborhoods with high radar roughness (SAR_Volume) through prohibiting solid vertical construction perpendicular to the prevailing wind direction (northwest). Designating longitudinal regression axes with the trees to allow for the dispersion of NO_2 gas and also the reduction of local global warming**.** Policy Frameworks where Baghdad Municipality's building code is being updated to include a green roof code for new commercial buildings. In parallel with declaring these densely populated thermal squares as Low-Emission Zones and the movement of heavy diesel vehicles is also restricted during peak summer hours. This will break the feedback loop between the chemical emissions and the heat islands.

Declaration of Competing Interest

The author declares that she has no known competing financial interests or personal relationships that could have appeared to influence the work reported in this paper.

REFERENCES

Al-Hashemi, H.M., Al-Sabbagh, Z.O., and Al-Hemidi, A.H., 2022. Assessment of land surface temperature and heat island in Baghdad city using Landsat data. *Arabian Journal of Geosciences*, 15(11), P. 1045. https://doi.org/10.1007/s12517-022-10141-8.

Al-Sabbagh, Z.M., and Al-Lami, A.K., 2021. Investigating the impact of urban morphology on sustainable city development: Baghdad as a case study. *Journal of Engineering*, 27(6), pp. 88-103. https://doi.org/10.31026/j.eng.2021.06.07.

Belgiu, M., and Drăguț, L., 2016. Random forest in remote sensing: A review of applications and future directions. *ISPRS Journal of Photogrammetry and Remote Sensing*, 114, pp. 24-31. https://doi.org/10.1016/j.isprsjprs.2016.01.011.

Chen, L., Wu, J., Zhang, L., Yang, S., and Wu, Z., 2023. Understanding 3D urban morphology and its impact on thermal environment using Sentinel-1 SAR and satellite imagery. *ISPRS Journal of Photogrammetry and Remote Sensing*, 198, pp. 115-130. https://doi.org/10.1016/j.isprsjprs.2023.03.012.

Ermida, S. L., Soares, P., Mantas, V., Göttsche, F. M., and Trigo, I. F., 2020. Google Earth Engine open-source code for Land Surface Temperature estimation from the Landsat series. *Remote Sensing*, 12(9), P. 1471. https://doi.org/10.3390/rs12091471

Fan, Y., Li, Y., Bechtel, B., Martilli, A., Giannaros, T.M., Zhang, Y., and Liu, L., 2023. Synergistic effects of air pollution and surface urban heat islands: A global perspective. *Science of The Total Environment,* 858, P. 159789. https://doi.org/10.1016/j.scitotenv.2022.159789.

Filipponi, F., 2019. Sentinel-1 GRD preprocessing workflow. *Proceedings*, 18(1), P. 11. https://doi.org/10.3390/ECRS-3-06189

Gao, Y., Zhao, J., and Han, L., 2022. Exploring the spatial heterogeneity of urban heat island effect and its relationship with 2D/3D urban morphology. *Building and Environment*, 208, P. 108579. https://doi.org/10.1016/j.buildenv.2021.108579.

Gorelick, N., Hancher, M., Dixon, M., Ilyushchenko, S., Thau, D., and Moore, R., 2017. Google Earth Engine: Planetary-scale geospatial analysis for everyone. *Remote Sensing of Environment*, 202, pp. 18-27. https://doi.org/10.1016/j.rse.2017.05.010.

Hafner, J., Katurji, M., Zawar-Reza, P., and Revell, L.E., 2024. Multi-sensor data fusion for urban climate monitoring: Challenges and opportunities. *Remote Sensing Applications: Society and Environment,* 33, P. 101124. https://doi.org/10.1016/j.rsase.2023.101124.

Haseeb, M., Al-Sabbagh, Z.O., and Al-Hemidi, A.H., 2026. Spatio-temporal interactions of air pollution, vegetation health, and land surface temperature: Insights from multi-sensor satellite observations. *Environment, Development and Sustainability*, pp. 1-32. https://doi.org/10.1007/s10668-026-07649-y

Hoang, N.D., and Nguyen, Q.L., 2025. Geospatial analysis and machine learning framework for urban heat island intensity prediction: Natural gradient boosting and deep neural network regressors with multisource remote sensing data. *Sustainability*, 17(10), P. 4287. https://doi.org/10.3390/su17104287

Jasim, L.K., Hasan, R.H., and Ibrahim, O.A., 2025. Evaluation of the accuracy of machine learning classifiers and spectral indices in land cover classification. *Engineering, Technology & Applied Science Research*, 15, pp. 22548–22552. https://doi.org/10.48084/etasr.10406.

Kaplan, G., Avdan, U., and Avdan, Z.Y., 2021. Nitrogen dioxide (NO2) monitoring using Sentinel-5P TROPOMI data over major European cities. *Environmental Pollution*, 268, P. 115913. https://doi.org/10.1016/j.envpol.2020.115913.

Kumar, R., Singh, S.N., Sharma, A., Srivastav, S.K., and Gupta, A.K., 2024. Deciphering the non-linear drivers of urban heat island intensity using machine learning and SHAP analysis. *Sustainable Cities and Society*, 102, P. 105214. https://doi.org/10.1016/j.scs.2024.105214.

Li, X., Zhou, W., and Ouyang, Z., 2021. Relationship between land surface temperature and spatial pattern of greenspace: What are the effects of spatial resolution?. *Landscape and Urban Planning*, 214, P. 104171. https://doi.org/10.1016/j.landurbplan.2021.104171.

Liu, X., Hu, G., Chen, Y., Li, X., Xu, X., and Li, S., 2024. A hybrid cloud-based framework for global urban climate modeling using Google Earth Engine. *Nature Communications*, 15, P. 432. https://doi.org/10.1038/s41467-024-44781-w.

Maxwell, A.E., Warner, T.A., and Fang, F., 2021. Machine learning in the geosciences: Challenges, opportunities, and implications. *Geoscientific Model Development*, 14(4), pp. 2031-2056. https://doi.org/10.5194/gmd-14-2031-2021.

Molnar, C., 2020. Interpretable Machine Learning: A Guide for Making Black Box Models Explainable. Leanpub.

Mullissa, A., Vollrath, A., Odongo-Braun, C., Slagter, B., Balling, J., Gou, Y., Gorelick, N., and Reiche, J., 2021. Sentinel-1 SAR backscatter analysis ready data preparation in Google Earth Engine. *Remote Sensing*, 13(10), P. 1954. https://doi.org/10.3390/rs13101954

Oke, T.R., Mills, G., Christen, A., and Voogt, J.A., 2017. *Urban Climates*. Cambridge University Press. https://doi.org/10.1017/9781139016476.

Parastatidis, D., Griffin, Z.M., Buyert, S., and Stalker, L., 2021. Monitoring the urban thermal environment: A review of the state-of-the-art. *Energy and Buildings*, 233, P. 110668. https://doi.org/10.1016/j.enbuild.2020.110668.

Ren, Z., Du, C., Han, X., He, X. and Pu, R., 2023. The synergistic effect of nitrogen dioxide and surface temperature on urban health risks: A remote sensing approach. *Remote Sensing*, 15(12), P. 3045. https://doi.org/10.3390/rs15123045.

Salman, S.A., Shahid, S., Ismail, T., Ahmed, A.S., and Wang, X.J., 2021. Analysis of heat island intensity in semi-arid cities: A case study of Baghdad. *Urban Climate*, 38, P. 100894. https://doi.org/10.1016/j.uclim.2021.100894.

Shrestha, A., Moore, N., and Ifaei, P., 2022. Identifying the drivers of urban heat island effect using random forest and permutation importance. *Sustainable Cities and Society*, 78, P. 103643. https://doi.org/10.1016/j.scs.2021.103643.

Sobrino, J.A., Jiménez-Muñoz, J.C., and Paolini, L., 2004. Land surface temperature retrieval from LANDSAT TM 5. *Remote Sensing of Environment*, 90(4), pp. 434-440. https://doi.org/10.1016/j.rse.2004.02.003

Sun, Y., Liu, X., Hu, G., Chen, Y., Li, X., and Li, S., 2022. Integration of Sentinel-1 SAR and Sentinel-2 optical data for urban morphology mapping. *International Journal of Applied Earth Observation and Geoinformation*, 107, P. 102681. https://doi.org/10.1016/j.jag.2021.102681.

Tamiminia, H., Salehi, B., Mahdianpari, M., Behmanesh, L., Mirmazloumi, S.M., and Brisco, B., 2020. Google Earth Engine for geo-big data applications: A meta-analysis and systematic review. *ISPRS Journal of Photogrammetry and Remote Sensing*, 164, pp. 152-170. https://doi.org/10.1016/j.isprsjprs.2020.04.001.

Tuholske, C., Caylor, K., Funk, C., Verdin, A., Sweeney, S., Grace, K., Peterson, P., and Evans, T., 2021. Global urban population exposure to extreme heat. *Proceedings of the National Academy of Sciences (PNAS), 118(41).* https://doi.org/10.1073/pnas.2024792118.

Tyralis, H., Papacharalampous, G., and Langousis, A., 2019. A brief review of random forests for predictions in hydrology and environmental sciences. *Water*, 11(5), P. 910. https://doi.org/10.3390/w11050910.

Ulpiani, G., 2021. On the linkage between urban heat island and outdoor air pollution: A review. *Science of The Total Environment*, 767, P. 144464. https://doi.org/10.1016/j.scitotenv.2020.144464.

Wang, J., Li, Y., 2023. Assessing the synergistic effects of urban heat island and air pollution: A spatiotemporal approach using Sentinel-5P and Landsat data. *International Journal of Applied Earth Observation and Geoinformation,* 118, P. 103239. https://doi.org/10.1016/j.jag.2023.103239.

Zhang, H., and Li, W., 2025. The polluted heat dome: Empirical evidence and theoretical framework for urban environmental health. *Science of The Total Environment*, 906, P. 167521. https://doi.org/10.1016/j.scitotenv.2024.167521.

Zhang, X., Wang, D., and Chen, H., 2024. Multi-sensor data fusion for urban microclimate modeling using machine learning. *ISPRS Journal of Photogrammetry and Remote Sensing,* 205, pp. 112-128. https://doi.org/10.1016/j.isprsjprs.2023.11.012.

تقييم التأثير التآزري للمورفولوجيا الحضرية وتلوث الهواء على الجزر الحرارية السطحية باستخدام الدمج متعدد المستشعرات والتعلم الآلي

رغد هادي حسن

قسم هندسة المساحة، كلية الهندسة، جامعة بغداد، بغداد، لعراق

الخلاصة

تواجه البيئات الحضرية تحديات مناخية كبيرة نتيجة للتوسع الحضري السريع، مما يُفاقم ظاهرة الجزر الحرارية الحضرية السطحية ويزيد من مخاطرها على الصحة العامة. تهدف هذه الدراسة إلى تجاوز الأطر التقليدية القائمة على مصادر بيانات منفردة، وذلك من خلال اقتراح إطار عمل هجين يعتمد على تقنية دمج البيانات من عدة مستشعرات ضمن بيئة الحوسبة السحابية لمحرك جوجل إيرث. غطى نطاق الدراسة مدينة بغداد خلال الفترة 2018–2023، حيث تم دمج بيانات الأقمار الصناعية (لاندسات 9/8، وسنتينل–1، وسنتينل–2، وسنتينل–P5) لاستخلاص متغيرات مورفولوجية وبيئية بدقة.لضمان تمثيل دقيق للمناخ المحلي على مستوى الأحياء وتقليل تأثيرات تداخل الرادار ، استخدم البحث منهجية توحيد قياسية، تلاها بناء نموذج مكاني–زماني متطور قائم على خوارزمية الغابة العشوائية لتقييم الأوزان النسبية للعوامل الحضرية المؤثرة. وقد أظهر النموذج كفاءة تنبؤية استثنائية واتساقًا إحصائيًا عاليًا، مسجلاً معامل تحديد ($R^2 = 0.842$) وخطأ معياري منخفض (RMSE = 1.007 درجة مئوية).أظهرت النتائج أن مورفولوجيا المدن (الممثلة بمؤشر المباني NDBI بنسبة 29.43%) وتدهور جودة الهواء (الممثل بتركيزات ثاني أكسيد النيتروجين بنسبة 25.38%) هما العاملان الرئيسيان في ارتفاع درجة حرارة سطح الأرض. تقدم هذه الدراسة أدلة تجريبية قوية على حدوث ظاهرة قبة الحرارة الملوثة، وتوفر لصناع السياسات أداة تحليلية فعالة لتقييم الصحة البيئية وتخطيط مدن أكثر مرونة واستدامة في مواجهة تغير المناخ الحاد.

الكلمات المفتاحية: تحليل الاستشعار عن بعد، الجزر الحرارية الحضرية السطحية، البيانات المكانية الضخمة، معالجة الصور، خوارزمية الغابة العشوائية